Title

Disruption of beta-catenin dependent Wnt signaling in colon cancer cells remodels the microenvironment to promote tumor invasion

Journal

Molecular Cancer Research, 20(3)

ISSN

1541-7786

Authors

Chen, George T
Tifrea, Delia F
Murad, Rabi
et al.

Publication Date

2022-03-01

DOI

10.1158/1541-7786.mcr-21-0349

Peer reviewed

HHS Public Access

Author manuscript

Mol Cancer Res. Author manuscript; available in PMC 2022 September 01.

Published in final edited form as:

Mol Cancer Res. 2022 March 01; 20(3): 468–484. doi:10.1158/1541-7786.MCR-21-0349.

Disruption of beta-catenin dependent Wnt signaling in colon cancer cells remodels the microenvironment to promote tumor invasion

George T. Chen[1], **Delia F. Tifrea**[2], **Rabi Murad**[3], **Amber N. Habowski**[1], **Yung Lyou**[1], **Madeleine R. Duong**[1], **Linzi Hosohama**[1], **Ali Mortazavi**[3], **Robert A. Edwards**[2], **Marian L. Waterman**[*,1]

[1]Department of Microbiology & Molecular Genetics, University of California, Irvine

[2]Department of Pathology, University of California, Irvine

[3]Department of Developmental & Cell Biology, University of California, Irvine

Abstract

The recent classification of colon cancer into molecular subtypes revealed that patients with the poorest prognosis harbor tumors with the lowest levels of Wnt signaling. This is contrary to the general understanding that overactive Wnt signaling promotes tumor progression from early initiation stages through to the later stages including invasion and metastasis. Here, we directly test this assumption by reducing the activity of ß-catenin-dependent Wnt signaling in colon cancer cell lines at either an upstream or downstream step in the pathway. We determine that Wnt-reduced cancer cells exhibit a more aggressive disease phenotype, including increased mobility *in vitro* and disruptive invasion into mucosa and smooth muscle in an orthotopic mouse model. RNA sequencing reveals that interference with Wnt signaling leads to an upregulation of gene programs that favor cell migration and invasion and a downregulation of inflammation signatures in the tumor microenvironment. We identify a set of upregulated genes common among the Wnt perturbations that are predictive of poor patient outcomes in early-invasive colon cancer. Our findings suggest that while targeting Wnt signaling may reduce tumor burden, an inadvertent side effect is the emergence of invasive cancer.

Introduction

Globally, colorectal cancer (CRC) is one of the leading causes of cancer-related deaths. Although increased screening, changes in lifestyle habits, and improvements in treatment have decreased the CRC mortality rate, metastatic disease continues to be a significant challenge to treat. Approximately 50-60% of CRC patients will develop metastatic disease,

[*]Corresponding author: marian.waterman@uci.edu, 839 Health Sciences Dr., Sprague Hall Room 240, Irvine, CA 92092, (949)824-2885.

Author contributions: GTC and MLW conceived of the experiments and wrote the manuscript. GTC and DFT performed the cell biology and animal experiments. GTC and YL created the cell lines and performed the experiments. GTC, ANH, MRD, LH, and DFT performed immunohistochemistry and imaging. RM and AM performed the orthotopic tumor sequencing and analysis. RAE and DFT performed the blinded pathology scoring and obtained all animal protocol approvals.

Competing interests: The authors have no competing interests to declare.

and the five-year relative survival for these patients is 13.9% (1). Mutations in the Wnt signaling pathway are a hallmark of CRC, with 80-90% of patients harboring pathway-activating mutations. The most common mutations in CRC target the tumor suppressor adenomatous polyposis coli (*APC*), which limits the ability of cells to sequester and degrade the Wnt effector ß-catenin. Stabilized ß-catenin can translocate to the nucleus for recruitment by LEF/TCF transcription factors to activate Wnt target gene expression. Although the general consensus is that *APC*-inactivating mutations chronically activate ß-catenin-LEF/TCF signaling and render CRC active and independent of Wnt ligands, recent evidence has shown that Wnt ligands are still capable of modulating Wnt activity, even in *APC*-mutant cells (2,3). The ability of Wnt ligands to modulate signaling in APC-mutant CRC is of particular interest, as both the tumor cells and the surrounding microenvironment express Wnt ligands throughout disease progression (4,5).

The general model for Wnt-driven CRC is that an overactive Wnt pathway drives disease progression through all stages. However, several studies have suggested that Wnt pathway activity may actually be lower in the most invasive forms of CRC and/or in the advanced, metastatic, chemoresistant, poor prognosis stages (6–8). One of these studies analyzed over 3,000 patient samples biopsied from the primary tumor site and associated clinical data to develop a categorization scheme of four subtypes. In their schema, tumors with the highest Wnt gene signature (labeled CMS2, or Canonical) exhibited the best overall clinical outcome, while the patients with the weakest Wnt signature (CMS4, or mesenchymal) exhibited invasive, poor prognosis disease. A separate effort to classify colorectal cancers analyzed 515 PDX tumors devoid of human stromal cells and identified five CRC/CRIS subtypes (9). Consistent with the CMS classification, subtypes with the strongest Wnt signaling (CRIS-C,-D,-E) had better prognoses than the subtypes with lower Wnt signaling activity (CRIS-A, -B). Using one or more of these classifications, multiple follow-up studies continue to reveal that the most aggressive subtypes of CRC are not the tumors with the highest levels of Wnt signaling. One study aligned PDX models and a large panel of colon cancer cell lines to the CMS system and revealed a clear difference in response to chemotherapy between CMS2 and CMS4 samples. While higher levels of expression of the Wnt target gene c-MYC has been connected to chemoresistance (10), chemotherapy treatment of cell lines cultured *in vitro* and/or injected subcutaneously in NSG mouse models revealed that the Wnt-lower CMS4 samples were more resistant to treatment (11). Importantly, this study showed that a majority of the traditional colon cancer cell lines tested (43 lines) could be classified into the four different CMS groups, even though these cells have been maintained in an *in vitro* system for decades. This suggests that there is at least some level of intrinsic stability of gene program expression in cancer cell lines that preserves CMS status *ex vivo* and in the xenograft setting. Higher resolution studies that analyzed gene expression at various CRC stages or small budding cell clusters at the invasive edge of primary tumors also observed a correlation with lower Wnt pathway activity (8,12).

While these correlative studies suggest that CRCs with moderate-to-low Wnt signaling are more aggressive, only a few studies have tested whether it is the weaker level of Wnt pathway activity that is linked to these phenotypic behavior differences in the primary tumor setting. One study has shown that repression of Wnt signaling through expression of dominant negative interfering LEF/TCF (dnTCF4) in CRC cell lines increased the ability of

cells to seed tumors in multiple tissues when introduced into mice via tail vein injection (13,14); another group deleted the TCF-4 gene (*TCF7L2)* in multiple CRC lines and observed a consistent change in morphology and invasive phenotypes (15). But these studies did not examine invasion phenotypes in the orthotopic setting of the colon where the primary tumor forms, nor were there any gene expression studies that might link these changes to CRC classification schemes and/or patient tumor data linked to outcomes.

Here we directly address these unknowns using two different approaches to genetically manipulate the level of Wnt/ß-catenin activity in colorectal cancer cells. We evaluate the tumor phenotype consequences of these manipulations via orthotopic xenografts in the mouse colon followed by histological and RNAseq analysis of both the human and mouse cell populations in the tumors. We observe that interference with Wnt signaling leads to an increase in tumor invasion. Comparing the differentially expressed genes between the parental and downregulated lines, we directly connect decreases in Wnt signaling with increased expression of secreted signals for cellular invasion from the cancer cells, and gene expression changes in the tumor microenvironment that indicate reduced inflammation. Specifically, we observe changes in the localization of microenvironment components in Wnt-reduced tumors that further illustrate a diminished immune response. We demonstrate that the gene expression changes observed in our model system are enriched in CMS4 patients from The Cancer Genome Atlas. Additionally, we identify signaling networks expressed in tumors that are significantly correlated with poor prognosis in multiple CRC patient datasets. We suggest that inhibition of Wnt signaling in Wnt-high colon tumors will lead to a dramatic increase in tumor invasion and aggression.

Materials and Methods

Cell lines

SW480, SW620, COLO320, and HCT116 were obtained from ATCC. Mycoplasma testing was conducted quarterly using the MycoAlert Mycoplasma Detection Kit (Lonza LT07-218). To authenticate cells, genomic DNA was submitted for short tandem repeat profiling and compared against the ATCC database annually. Cell lines were cultured in Dulbecco's Modification of Eagle's Medium (DMEM, Hyclone) or RPMI-1640 (Hyclone) supplemented with 10% Fetal Bovine Serum (Atlas Biologicals), 1% Penicillin/Streptomycin (Mediatech), and 2mM Glutamine (Mediatech). Unless otherwise stated, all assays were conducted in the same media. dnLEF1 cell lines were prepared as previously described (16). LRP6 knockout (LRP6KO) cell lines were created by co-transfecting cell lines with 3 μg LRP6 CRISPR and 300 ng eGFP-Puro using BioT transfection reagent (Bioland Scientific, B01). After selection with Puromycin, cells were sorted for LRP6 knockdown using flow cytometry (anti-human LRP6-APC, R&D Systems MAB1505, RRID:AB10889810) and successful knockdown was confirmed by Western blot.

LRP5 and LRP6 CRISPR constructs

The CRISPR kit used for constructing multiplex CRISPR/Cas9 vectors was a gift from Takashi Yamamoto (Addgene kit #1000000054). Guide RNAs targeting LRP5 and LRP6 were designed using the Zhang Lab Optimized CRISPR Design Tool (http://crispr.mit.edu).

A Cas9 nickase system was used such that two closely aligned guides per gene were developed.

For LRP5, the primer pairs used were:

LRP5-Cas9n-1-Fwd: CACCGCTCGGTCCAGTAGATGTAGC,

LRP5-Cas9n-1-Rev: AAACGCTACATCTACTGGACCGAGC,

LRP5-Cas9n-2-Fwd: CACCGCGGCAAGCCGAGGATCGTGC,

LRP6-Cas9n-2-Rev: AAACGCACGATCCTCGGCTTGCCGC.

For LRP6, the primer pairs used were:

LRP6-Cas9n-1-Fwd: CACCGTTGGCCAAATGGTTTAGCCT,

LRP6-Cas9n-1-Rev: AAACAGGCTAAACCATTTGGCCAAC,

LRP6-Cas9n-2-Fwd: CACCGAAGTGTTAACCAATACTACA,

LRP6-Cas9n-2-Rev: AAACTGTAGTATTGGTTAACACTTC.

Guides were inserted into vectors using T4 polynucleotide kinase (New England Biolabs), and the final combined guide RNA vector was assembled by Golden Gate Assembly using Quick Ligase (New England Biolabs). The final vector was electroporated into DH5α competent cells and purified using a Nucleospin Maxiprep kit (Macherey Nagel). Restriction enzyme digested products were run out on an agarose gel to confirm insert size and plasmid quality. Correct assembly was verified by Sanger Sequencing.

LRP5 and LRP6 shRNA

LRP5 & LRP6 shRNA constructs were obtained from the RNAi Consortium database (Sigma Aldrich). Lentivirus was packaged in HEK293T cells (ATCC) and purified using PEG-it (System Biosciences).

Western blotting

Whole cell lysates were prepared by resuspending a cell pellet in an appropriate amount of RIPA buffer containing protease inhibitors and phosphatase inhibitors and incubating for 30 minutes on ice. The lysates were spun down at high speed for 15 minutes at 4C, and the supernatant was transferred to a clean tube. Lysates were quantified using a Bradford assay (BioRad, 500-0205). 80 μg of total cell lysates were analyzed by Western blot using the following antibodies and concentrations: LRP6 (1:1000, Cell Signaling Technology 3395, RRID:AB1950408), LRP5 (1:1000, Cell Signaling Technology 5731, RRID:AB_10705602), ß-Catenin (1:1000, Cell Signaling Technology 8480, RRID:AB_11127855), ß-Tubulin (1:2000, Genetex GTX101279, RRID:AB_1952434). All blots were incubated overnight in primary antibody, washed, and then incubated for two hours in secondary antibody – anti-rabbit-HRP (1:5000, GE Healthcare) or anti-mouse-HRP (1:2000, GE Healthcare). Blots were imaged using a Syngene G-Box system. Bands were quantified using Adobe Photoshop (RRID:SCR_014199). Statistical evaluation of three or more independent biological replicates was performed using Student’s unpaired T-Test.

Luciferase assay

Cells were seeded at a density of 1 *10^5 cells per well in a 12-well tissue culture plate using antibiotic-free media 24 hours prior to transfection. Cells were co-transfected with 100ng Wnt ligand expression plasmid (17), 300ng LRP5 or LRP6 CRISPR construct, 100ng SuperTOPFlash or SuperFOPFlash (Gifts from Dr. R.T. Moon, Addgene plasmid 12456) and 100ng CMV-ß-Galactosidase using BioT (Bioland Scientific B01-02) per manufacturer's instructions. Cells were harvested 24 hours post-transfection and assayed for luciferase activity and ß-galactosidase activity (as a normalization control). Statistical evaluation was performed using Student's unpaired T-test.

Scratch assay

Cells were seeded at a density of 2*10^6 cells per well in a 6-well plate. After 24 hours, 2 crosses were scratched into the cell monolayer with a P1000 tip. Each well was washed once with PBS before incubating in media. Images were taken at 0 hours, 24 hours, and 48 hours post-scratch. Measurements were obtained using Adobe Photoshop image analysis. Statistical evaluation was performed using Student's unpaired T-test.

Flow cytometry

One million cells per sample condition were collected and washed with FACS buffer (3% FBS in PBS). If needed, cells were fixed in 4% paraformaldehyde for 15 minutes at room temperature, permeabilized by 0.1% saponin in HBSS for 15 minutes on ice and washed twice with FACS buffer prior to staining. Cells were incubated with primary antibody for 1 hour at room temperature in the dark. If secondary antibody was needed, cells were washed twice with FACS buffer prior to incubating in secondary antibody for 30 minutes at room temperature, in the dark. Cells were finally washed and resuspended in 300-600 µL FACS buffer per sample and analyzed on either a BD FACSAria or Acea Biosciences Novocyte. Data was analyzed using FlowJo (Treestar, RRID:SCR_008520).

Clonogenic assay in fibrin

Briefly, 200 trypsinized cells were mixed with 100µL of 2.5 mg/mL bovine fibrinogen (MP Biomedicals) in DMEM plus 10% FBS and 1% Penicillin-Streptomycin-Glutamine and 1µL of thrombin (Sigma). The fibrin gels were seeded in 96 well, flat bottom plates. After the gels solidified, 100µL of DMEM media was layered on top. Wells were imaged regularly up to 14 days. Size measurements were taken using Adobe Photoshop. Data was analyzed using Prism (Graphpad, RRID:SCR_002798).

Orthotopic injections

Immuno-deficient NSG mice (Jackson Labs) were anaesthetized with 300µl of 100mg/kg ketamine/10mg/kg xylazine. The surgical site was shaved and cleaned with ethanol. After an incision was made, the caecum was drawn out and washed with sterile PBS. Cells (5*10^5) were injected in the caecum wall at six to eight sites using a Hamilton syringe (Hamilton 80301), three to four injections per side. The peritoneal wall and skin were sutured separately, the former with resorbable sutures, the latter with nylon. 5mg/kg carprofen was injected as an analgesic. Mice health was monitored for 28 days prior to harvest. The

University of California Irvine IACUC approved all animal experiments under protocol #AUP-17-053.

Mesentery dissociation for flow cytometry

Mesentery from orthotopically-injected mice were collected in a petri dish on ice and briefly diced with razor blades before transferring the tissue pieces into a 40 micron strainer and pushing tissue through the strainer using the plunger of a 3ml syringe. The strainer was rinsed with 10ml DMEM with 5% FBS, 1% P/S, and 2mg/ml Collagenase I (Sigma). The mixture was collected in a conical tube and shaken at 37 C for 1 hour. The tube was spun down and the supernatant aspirated. The pellet was washed in 10ml HBSS, spun down, and supernatant aspirated except for approximately 500 μl of HBSS. 50 μl DNAse I (10 U, Thermo Fisher) was added and the pellet resuspended and incubated at room temperature for five minutes. Following DNAse treatment, 2 ml of 0.05% trypsin was added, and the mixture was incubated at 37 C for 10 minutes. 5 ml DMEM with 5% FBS was then added, the mixture spun down, and the supernatant was aspirated. The pellet was resuspended in 5 ml DMEM and passed through a 40-micron cell strainer. The strainer was washed with an additional 5 ml of DMEM and the cell number and viability was measured using a Countess II (Thermo Fisher Scientific). $1*10^6$ cells per sample were incubated in CD298-APC (Miltenyi Biotec, RRID:AB_2657030) for one hour at room temperature in the dark. Samples were washed twice in FACS buffer before resuspending in FACS buffer and running on an Acea Biosciences Novocyte. Data was analyzed using FlowJo (Treestar).

Subcutaneous injections

Immuno-deficient NSG mice (Jackson Labs) were anaesthetized with 300μl of 100mg/kg ketamine/10mg/kg xylazine. The surgical site was shaved and cleaned with ethanol. $2*10^6$ cells were resuspended in 100 μL PBS and injected under the skin on both flanks of the mouse. Mice health was monitored for 21 days prior to harvest.

Immunohistochemistry

Excised caecums were fixed in 10% formalin for 24 hours, cut on the latitude, and mounted on edge in paraffin. 10 μm formalin-fixed paraffin-embedded (FFPE) sections were cut onto SuperFrost Plus (Fisher) slides. For Trichrome staining, the microwave staining protocol from the manufacturer was followed (Thermo Scientific 87019 – Masson Trichrome Stain Kit) with the following variations: maximum time for all deionized water rinses, 10 min Biebrich Scarlet-Acid Fuchsin stain, 7 min Aniline Blue stain followed by an addition deionized water rinse before acetic acid. Following alcohol dehydration and clearing with xylene, Trichrome stained slides were mounted with Permount mounting medium (Fisher SP15-100). For antigen retrieval, slides were deparaffinized and rehydrated, followed by antigen retrieval in a pressure cooker using the optimized buffer for each antibody (specified below) for five minutes at pressure. For H&E, slides were then stained by hematoxylin and eosin, dehydrated, and mounted using Permount mounting medium. For antibody staining following antigen retrieval, slides were blocked in 3% H_2O_2, goat serum, and then avidin and biotin blocking reagents (Vector Labs SP-2001). Sections were incubated in primary antibodies: Cleaved Caspase 9 (Thermo Fisher Scientific - MA5-32028, RRID:AB_2809322; 1:300), F4/80 (Abcam – ab111101, RRID:AB_10859466; 1:100 4 °C

overnight incubation; 10 mM pH 6 sodium citrate retrieval buffer), Ki-67 (Thermo Fisher Scientific - MA5-14520, RRID:AB_10979488; 1:200), Ly6g (Abcam – ab238132; 1:500 4 °C overnight incubation; 10 mM pH 8 tris EDTA retrieval buffer), and SMA1 (Abcam – ab5694, RRID:AB_2223021; 1:250 RT for 30 min; 10 mM pH 6 sodium citrate retrieval buffer). A biotinylated secondary antibody was used (goat-anti-rabbit; 1:200; VectorLabs BA-1000-1.5) and visualization using a peroxidase-conjugated avidin-based Vectastain protocol (ABC Elite - VectorLabs PK-4001; DAB Quanto – Fisher TA060QHDX). Slides were then counterstained with hematoxylin and mounted using Permount mounting medium. Whole slides scans of IHC antibody staining and Trichrome stained were performed with a Roche Ventana DP 200 slide scanner and then analyzed using QuPath (18). H&E slide images were captured with a Keyence BZ-X700 system and processed in Adobe Photoshop.

Pathology scoring

A blinded evaluation of stained slides was performed by pathologists who scored each section of caecum on the absence, low presence, or high presence of phenotypic features. Additional measurements were taken of each section by comparing the total pixels of a section to pixels of individual components (eg. extracolonic tumors, intact epithelia, et cetera) and normalizing by percentage of total section. To quantify positively stained cells in specific regions, equal sized frames were captured from tumor, stroma, and epithelial of each orthotopic tumor sample. Positive cells were counted from each frame and frames averaged for each condition and region type. To quantify positively stained cells overall, we used QuPath to create $250um^2$ annotations over a region of interest, only considering annotations which entirely encompassed a tissue. Cell detection was done using the automated QuPath tool targeting the hematoxylin stain; positive cells marked using the object classifier tool. The same classifier settings were used for all slides stained with the same antibody. Approximately three to five sections per caecum from at least three mice per cell line were analyzed. The complete set of analyzed images is in Supplemental Materials Figure 1.

Total RNA Isolation

RNA was extracted from cells using TRIzol (Invitrogen) and DirectZol RNA Extraction Kit following the manufacturer's instructions (Zymo Research). RNA was extracted from flash-frozen tissue samples by using a mortar and pestle to crush tissue into fine powder, homogenizing in TRIzol using a Precellys 24 (Bertin), and extracting the RNA with the DirectZol kit. RNA quality was checked with Agilent Bioanalyzer. Samples with RNA Integrity Number (RIN) scores ≥ 9 were used for RNA-seq library construction.

Quantitative PCR

RNA was extracted from cells using TRIzol (Invitrogen) and DirectZol RNA Extraction Kit following the manufacturer's instructions (Zymo Research). RNA was extracted from flash-frozen tissue samples by using a mortar and pestle to crush tissue into fine powder, homogenizing in TRIzol using a Precellys 24 (Bertin), and extracting the RNA with the DirectZol kit. cDNA was synthesized from 1 μg of total RNA using the High Capacity cDNA Reverse Transcription Kit (Invitrogen), as per the manufacturer's instructions. qPCR was performed in triplicate for each experimental condition using Maxima SYBR Green

qPCR Master Mix (Invitrogen), according to the manufacturer's instructions. Primer pairs used are as follows:

AXIN2: Forward: CTGGCTTTGGTGAACTGTTG Reverse: AGTTGCTCACAGCCAAGACA,

MYC: Forward: CTACCCTCTCAACGACAGCA Reverse: AGAGCAGAGAATCCGAGGAC,

SP5: Forward: AATGCTGCTGAACTGAATAGA Reverse: AACCGGTCCTAGCGAAAACC,

GAPDH: Forward: TCGACAGTCAGCCGCATCTTCTT Reverse: GCGCCCAATACGACCAAATCC.

Library Construction

RNA-seq libraries were built using the Smart-seq2 protocol (19) with modifications according to (20). Briefly, for each sample 10 ng of total RNA was converted to full-length cDNA using poly-dT primer and reverse transcriptase. The full-length cDNA was amplified using nine PCR cycles. 18 ng full-length cDNA for each sample was converted to sequencing library by tagmentation using the Illumina Nextera kit. Eight PCR cycles were used for library amplification. The libraries were multiplexed and sequenced on an Illumina NextSeq500 sequencer as 43 bp paired-end reads.

Sequencing Analysis

Adapter sequences and low quality base pairs from the 5' and 3' ends of the paired-ends reads were trimmed using Trimmomatic v. 0.35 (21) using the following parameters: "PE read1.fastq read2.fastq pe_read1.fastq.gz se_read1.fastq.gz pe_read2.fastq.gz se_read2.fastq.gz ILLUMINACLIP:NexteraPE-PE.fa:2:30:8:4:true LEADING:20 TRAILING:20 SLIDINGWINDOW:4:17 MINLEN:30". For each sample, the reads from the host (mouse) and the graft (human) were classified and separated using Xenome (22). Xenome outputs five classes of reads: host, graft, ambiguous, both, and neither. Only the host and graft reads were kept for mapping to the host and graft transcriptomes respectively while the other three classes of reads (ambiguous, both, and neither) were discarded.

We used GENCODE v. 28 reference transcriptome for human and GENCODE v. M18 for mouse (23). RNA-seq reads for each sample were mapped to the reference transcriptome using Bowtie v. 1.2 (24) with the following parameters: "-X 2000 -a -m 200 -S --seedlen 25 -n 2 -v 3". Gene expression levels and read counts were obtained using RSEM v. 1.2.31 (25).

Differential Gene Expression Analysis

Differential gene expression analysis was performed using DESeq2 R package (26). Gene ontology was performed using ShinyGO (27), and visualized using the iGraph R package (28). Gene Set Enrichment Analysis (GSEA) was performed using the GSEA software from the Broad Institute (29).

Patient survival analyses

Differentially expressed genes of secreted factors were input into STRING (30) to identify known interactors. Interactors found to be differentially expressed in our datasets were considered for Kaplan-Meier analysis. Only genes which demonstrated a change in survival between high expression and low expression of the gene were considered for the combined gene signatures. Kaplan-Meier analyses of publicly available colon cancer datasets TCGA-COAD (https://www.cancer.gov/tcga), GSE17538 (31), GSE39582 (32), and GSE41258 (33) were performed using Prism (Graphpad). For combined gene signatures, each gene's expression was considered individually and bifurcated at the median. The resulting "high expression" and "low expression" patient sets were overlapped for all genes to define a group of patients with high or low expression for all considered genes.

Data and materials availability

The data discussed in this publication have been deposited in NCBI's Gene Expression Omnibus (64) and are accessible through GEO Series accession number GSE130236. Plasmids used for CRISPR editing will be available through Addgene.

Results

Decreasing Wnt signaling in SW480 cells increases cell invasiveness

Our previous studies determined how decreases in Wnt signaling affect tumor progression in a subcutaneous xenograft tumor model (16). To decrease Wnt signaling, we lentivirally transduced an expression vector for dominant negative LEF1 (dnLEF1) into SW480 colon cancer cells prior to subcutaneous injection (Figure 1A–D). *LEF1* is a LEF/TCF transcription factor that binds to Wnt Response Elements (WREs) in enhancers and promoters and recruits ß-catenin to activate transcription of Wnt target genes. The dnLEF1 expression construct lacks coding sequences for the N-terminal ß-catenin binding domain, but retains all other sequences, including the HMG-box DNA binding domain and nuclear localization signal. This truncated transcription factor can localize to the nucleus and displace endogenous full-length LEF/TCFs from their occupancy of Wnt Response Elements (WREs) at bona fide Wnt target genes. We used this mode of interference as it had been first developed by Van de Wetering and Clevers to effectively interfere with canonical Wnt signaling in the nucleus (34). Indeed, using a Wnt-luciferase assay, we find that dnLEF1 transduction-expression decreases Wnt signaling activity by 80-90% compared to Mock-transduced cells in SW480 (Figure 1A). Expression of Wnt target genes *AXIN2*, *MYC*, and *SP5* are decreased with dnLEF1 transduction, as measured by quantitative PCR (Figure 1B). Three weeks after subcutaneous injection of transduced cells, we harvested the tumors and examined them histologically. We observed that tumors expressing dnLEF1 exhibited a significant seven-fold decrease of in tumor weight and volume (Figure 1C–D)(16). These data are in line with the overall understanding that high levels of Wnt signaling promote tumor growth and development. However, the subcutaneous microenvironment on the back flank of a mouse is not the endogenous location for colon tumor development and further, the subcutaneous environment lacks the nutrient availability of the richly vascularized intestinal epithelium. We therefore expanded our animal studies to include an orthotopic injection model whereby tumors were developed in the mouse colon.

To study tumorigenesis in a more representative microenvironment, we injected the SW480 Mock or SW480 dnLEF1 cells into the stroma between the epithelial and muscle wall layers of the caecum (Figure 1E–F). After four weeks of development, the caecums were harvested and sectioned for immunohistochemistry. Unlike our findings with subcutaneous tumors, we observed no gross deficit in tumor size when comparing the SW480 Mock and SW480 dnLEF1 orthotopic tumors, implying that the high-density vasculature in the colon wall was able to compensate for the deficits in angiogenic development in the subcutaneous-dnLEF1 tumors (Figure 1F–G). A blinded evaluation of physiological features for each tumor by pathologists revealed that SW480 dnLEF1 orthotopic tumors exhibit significantly higher rates of invasion into the submucosa and mucosa, higher prevalence of intratumor necrosis, and higher numbers of extracolonic tumors (tumors present on the exterior of the colon wall) (Figure 1H, full images with key in Supplemental Figure 1). *In vitro*, the SW480 dnLEF1 cells were significantly more migratory after 24 and 48 hours, as measured by a scratch assay (Supplemental Figure 6B). These data very clearly suggest that SW480 dnLEF1 tumors are more invasive and their cells more migratory.

The SW480 cell line was derived from the primary tumor of a CRC patient, and a metastatic lymph node from the same patient was used to derive the line SW620. It is known that SW620 cells have significantly less Wnt activity than SW480 (e.g. SW620 is closer in Wnt activity levels to SW480 dnLEF1 than SW480, Supplemental Figure 6A), and it is closely aligned with the invasive CMS4 subtype (11). We therefore predicted that SW620 tumors would have intrinsic, invasive phenotypes when developed orthotopically. In addition, we tested whether further reduction of Wnt signaling in this cell line would enhance invasion characteristics. Lentiviral transduction of the dnLEF1 construct into SW620 cells further reduced Wnt signaling levels (Figure 1I), and as with SW480 dnLEF1 cells, SW620 dnLEF1 showed significant or near significant decreased expression of Wnt target genes *AXIN2*, *MYC*, and *SP5* (Figure 1J). Also, consistent with our predictions in the orthotopic setting, SW620 Mock tumors are inherently invasive, and SW620 dnLEF1 tumors appeared to be even more aggressive (Figure 1K). Blinded evaluation of SW620 orthotopic tumors showed significant increases in incidence of extracolonic SW620 dnLEF1 tumors compared to SW620 Mock (Figure 1L). In both SW620 Mock and SW620 dnLEF1 tumors, more sections contained necrotic areas compared to SW480 Mock or SW480 dnLEF1 suggesting an innate, higher sensitivity of the SW620 cells to nutrient levels in the surrounding microenvironment. Using CD298 as a marker of human cells, we used flow cytometry analysis to detect human cancer cells that had migrated to neighboring mesenteric tissue (35). This analysis showed that a significantly higher percentage of CD298+ cells were present in the mesentery of orthotopically-injected SW620 dnLEF1 mice compared to SW620 Mock-injected mice, indicating a higher level of intravasation into the surrounding lymphatic network (Figure 1L) even though a decrease in local lymphatic invasion was observed. These data suggest that even in cell lines with low Wnt signaling activity, the effect of further decreasing Wnt activity creates a more aggressive tumor.

LRP6 is required for Wnt ligand:receptor signaling in colon cancer cells

Several groups have reported that Wnt ligands are capable of enhancing Wnt signaling activity, even in APC-mutant colon cancers (2,3,36–38). We hypothesized that autocrine-

acting Wnt ligands from the cancer cells and paracrine Wnt signals from the surrounding microenvironment might contribute to maintaining colon cancer cells in a non-invasive state in the orthotopic condition. The dominant negative LEF1 constructs do not directly address this hypothesis, as their effect is to interfere with ß-catenin actions in the nucleus, not the cell membrane. Therefore, to more directly probe how Wnt ligands in the tumor microenvironment affect ß-catenin-dependent signaling and colon cancer cell behavior, we used a CRISPR/Cas9 system to genetically delete the essential Wnt ligand co-receptors LRP5 (Supplemental Figure 2A) and LRP6 (Figure 2A). We tested the efficacy of this manipulation by transiently co-transfecting HEK293 cells with the Cas9 nickase, LRP5 or LRP6 guide RNA expression constructs, and various Wnt ligand expression plasmids for ligands known to be expressed in colon cancer. Using the SuperTOPFlash luciferase reporter, we assayed for Wnt signaling activity. Knockdown of LRP5 or LRP6 expression effectively interfered with Wnt ligand activation of the luciferase reporter. For example, we noted that the Wnt1 ligand required both LRP5 and LRP6 for reporter activation (Supplemental Figure 2B), in line with observations from other groups (39). We tested other Wnt ligands and found that while a number of Wnt ligands required both LRP5 and LRP6, others required solely LRP6, while none of the ligands required only LRP5 (Supplemental Figure 2C). In part, this may be due to LRP6 influencing LRP5 expression, as the knockout of LRP6 also reduced LRP5 protein (Supplemental Figure 3A & 3D). To confirm that this was not an off-target effect of our chosen guide RNAs, we also silenced LRP6 using an shRNA construct, which yielded the same result (Supplemental Figure 3B–D). Given that the LRP6 co-receptor appears to be a uniformly required co-receptor for ß-catenin-dependent signaling, we focused our remaining efforts using LRP6 knockout cells.

LRP6 modulates Wnt signaling levels in APC-mutant colon cancer

We noted that SW480 cells do not innately express much LRP6 protein and that what residual LRP6 protein is detectable, is not located on the cell membrane where Frizzled receptors reside (Figure 2B, Supplemental Figure 3E–G). Additionally, we found LRP6 expression to be only modestly decreased in dnLEF1-expressing SW480 and SW620 lines (Supplemental Figure 3 H& I), indicating that it is not a direct Wnt target. We therefore focused our LRP6 knockout efforts on SW620 cells because LRP6 is robustly expressed on the cell surface. Using flow cytometry, we isolated a population of LRP6 knockout cells from the total transfected SW620 cell population (Figure 2B). We validated that LRP6 expression is strongly decreased in SW620 LRP6KO cells by Western blot (Figure 2C–D). Interestingly, Wnt signaling is decreased by ten to twenty percent compared to expression of Cas9 alone (Figure 2E). However, as expected, compared to the dominant negative LEF1-expressing lines, the effect of a genetic LRP6 knockout on overall Wnt signaling in SW620 cells is not as strong (Figure 2E–F). These results demonstrate that decreasing expression of LRP6 decreases Wnt signaling only to a moderate level, pointing to real possibilities for ligand-based Wnt pathway activation, even in the presence of a downstream APC mutation. Additionally, we found that ß-catenin protein levels significantly decreased when *LRP6* was deleted, but not with dnLEF1 expression (Figure 2G–H). This decrease cannot be explained by a decrease in ß-catenin (*CTNNB1*) mRNA expression (Figure 2I), suggesting that ß-catenin protein degradation is enhanced. This is in line with findings from Saito-Diaz et al (40), who suggest that LRP6 associates with the ß-catenin

destruction complex in the absence of a Wnt ligand, partially inhibiting its activity. Thus, the loss of LRP6 allows the destruction complex to be more active, decreasing overall ß-catenin protein. We confirmed this by decreasing LRP6 expression in colon cancer cell line HCT116, which has a mutant ß-catenin and wildtype APC. *LRP6* knockout did not significantly decrease Wnt signaling activity in these cells, suggesting that the release of the destruction complex from the plasma membrane did not increase ß-catenin degradation (Supplemental Figure 4A). Interestingly, when we decreased LRP5 or LRP6 expression in colon cancer cell line COLO320, which has a highly truncated APC, we find that Wnt signaling is reduced by 40-50% (Supplemental Figure 4B). However, ß-catenin expression is not significantly reduced in LRP6-diminished cells, due to the absence of APC domains that interact with LRP6 (Supplemental Figure 4C–D). We conclude that removal of LRP6 in APC-mutant colon cancer cell lines destabilizes ß-catenin and moderately decreases Wnt signaling.

Loss of LRP6 enhances aggressive tumor phenotypes

In vitro, SW620 LRP6KO cells were more migratory than SW620 Cas9, but this enhanced phenotype was only significantly evident after 48 hours (Figure 2J). By contrast, SW620 dnLEF1 cells were significantly more migratory after 24 hours. Orthotopic tumors of SW620 Cas9 and SW620 LRP6KO were largely indistinguishable from one another by pathology scoring, except for the size of extracolonic tumors in LRP6KO sections (Figure 2K, L and Supplemental Figure 1). While the number of extracolonic tumors per section was similar between the two tumor types, the size of the LRP6KO extracolonic tumors were dramatically larger than the Cas9 tumors (Figure 2L), suggesting that the SW620 LRP6KO cells have an enhanced ability to develop into tumors outside the colon. Additionally, orthotopic tumors from COLO320 LRP6KO cells showed significantly increased necrosis and lymphatic invasion, in line with our observations with the SW480 and SW620 tumors, though interestingly this line did not show any extracolonic tumors (Supplemental Figure 4E). This suggests that there may be a graded effect to Wnt signaling inhibition of cell migration, with decreasing Wnt signaling levels yielding a graded increase in invasion. Using immunohistochemical staining approaches, we probed orthotopic tumors for phosphorylated Histone H3 as a marker of mitosis, Ki67 as a marker of active cell cycling, and cleaved Caspase 9 as a marker of apoptosis. We found no measurable difference in phospho-histone H3 and caspase 9 positivity between the two tumor types, but significantly higher levels of Ki67 positivity in SW620 LRP6KO orthotopic tumors compared to the SW620 Cas9 control tumors (Supplemental Figure 3J). Interestingly, we observed high Caspase 9 positivity in the stroma of the parental SW620 tumors but very little evidence of Caspase 9 positivity in the human cancer cells of either tumor type. We conclude that while the larger SW620 LRP6KO extracolonic tumors could derive from earlier migration of SW620 LRP6KO cells, their larger size is due at least in part to a greater proportion of actively cycling cells.

Suppression of ß-catenin-dependent Wnt signaling in cancer cells leads to changes in signatures of invasion and inflammation

To identify changes in gene expression that occur in the conversion to an invasive phenotype, we performed RNAseq of bulk mRNA from the orthotopic tumors, taking

advantage of the mixed mouse and human cell environment to analyze concurrent gene expression changes in the human tumor versus the mouse stroma. We also used the percentage of reads mapped to human versus mouse genomes to serve as a proxy for assessing the relative abundance of human versus mouse tissue (Figure 3A). We found that overall, the Wnt-low, SW620 tumor cells (both control and further Wnt-diminished), comprised a higher percentage of the tissue samples than the SW480 tumors, with PBS-injected caecums serving as a negative control. Differential gene expression analysis revealed approximately 350 significantly changed genes in SW480 dnLEF1 cells compared to SW480 Mock, but twice as many significant changes in the SW620 Mock versus SW620 dnLEF1. Not surprisingly, the more moderate change in Wnt signaling induced by knocking out LRP6 led to fewer and smaller, but still-significant changes in gene expression in SW620 (Figure 3B). We compared the expression of classical markers of epithelial-to-mesenchymal transition (EMT) in the matching tumor types and observed a trend of decreasing epithelial gene expression and increasing mesenchymal gene expression in the Wnt-reduced tumors, although few of these changes reached significance (Figure 3C). Additionally, as poorly differentiated tumors are known to be more invasive than well-differentiated tumors, we evaluated the expression of stemness and differentiation associated genes and found significant upregulation of stemness genes *FOXP1* and *SMOC2* in SW480 dnLEF1 cells, and significant downregulation of differentiation genes *CDX2* and *SHH* (Figure 3D). We observed a similar trend in the SW620 tumor types; however, the gene expression changes did not reach significance (Figure 3D). For an *in vitro* test, we used clonogenic assays to assess if emergent properties of stemness were more evident in SW480 dnLEF1 or SW620 dnLEF1 cultures. We did not observe any significant differences in number of colonies or size of colonies when comparing dnLEF1-expressing lines to Mock-expressing controls, suggesting that the observed expression changes in stemness associated genes are not sufficient to impart an overt, dominant change in stemness-relevant phenotypes (Supplemental Figure 3K & L).

We additionally performed RNAseq on bulk mRNA from *in vitro* CRC cultures to compare gene expression to the orthotopic samples. Differential gene expression analysis showed the greatest number of significant changes when comparing SW480 dnLEF1 and SW480 Mock; fewer changes were observed in SW620 dnLEF1 and the fewest number of genes were significantly changed in SW620 LRP6KO (Supplemental Figure 5A, 6A). Many of the significantly upregulated genes in the orthotopic tumors were also upregulated *in vitro* (Supplemental Figure 5B, 6E). Using Gene Set Enrichment Analysis (GSEA (41)), we found that Wnt target genes linked to colon cancer were significantly enriched in SW480 Mock compared to SW480 dnLEF1 (Supplemental Figure 5C). Using Gene Ontology (GO) analyses, we observed that gene programs related to extracellular matrix, cell adhesion, and cell migration were significantly changed by Wnt interference in both the *in vitro* and tumor data, suggesting that there are innate changes that drive the increased cell migration phenotypes (Supplemental Figure 5D). As with the orthotopic tumors, a decrease in differentiation marker expression and a trend towards EMT was most significant in SW480 dnLEF1 (Supplemental Figure 6D). Using immunoblotting, we found upregulation of two markers of EMT, AXL and Vimentin, supporting our transcriptomic findings (Supplemental Figure 6F–G). Given the lack of overt changes in stemness phenotypes in the SW480

dnLEF1 tumors and lack of significant changes in stemness, differentiation, and EMT markers in the SW620 cell lines (Supplemental Figure 6C), we focused our downstream analysis on the SW480 dominant negative LEF1-expressing cells and cell communication programs directed toward the tumor microenvironment.

To compare SW480 dnLEF1 and SW480 Mock orthotopic tumors, we performed GO analyses on significantly upregulated and downregulated genes and clustered the GO terms by shared function and list members (Figure 3E; *in vitro* Supplemental Figure 6H). The resulting clusters revealed an upregulation of GO terms associated with extracellular and intracellular signaling, and a downregulation of terms associated with cell differentiation and morphogenesis. We were particularly interested in the role that extracellular signaling may play in advancing tumor invasion given the literature showing APC-mutant cancer cells respond to stimulation from Wnt ligands. Thus, we looked at the expression fold change of all known genes for secreted proteins (Figure 3F). Many of the genes that are significantly upregulated in the SW480 dnLEF1 tumors encode secreted proteins with known functions in cell migration, and many of the most significantly downregulated genes encode inflammatory mediators, suggesting that the Wnt-reduced cancer cells were eliciting a reduced immune response relative to the parental SW480 Mock tumors.

Suppression of ß-catenin-dependent Wnt signaling in cancer cells leads to a less inflamed microenvironment

To determine if the murine tumor microenvironment reacted differently to the two tumor types, we compared the expression of genes in sham-injected, SW480 Mock-injected, and SW480 dnLEF1-injected mouse stroma. As a ground truth, we performed GO analysis on significantly upregulated and downregulated genes in stromal cells comparing SW480 Mock injection to sham injection. Unsurprisingly, the GO terms that emerge in response to a tumor is clustered on programs of immune response and extracellular matrix remodeling (Figure 4A). We then looked for tumor microenvironment gene expression differences when a SW480 Mock tumor is growing in the intestine versus a SW480 dnLEF1 tumor. We found that there is a significant downregulation in immune response GO terms (Figure 4B; against sham Supplemental Figure 7B), indicating that the downregulated inflammatory signals from the human SW480 dnLEF1 cancer cells appear to be met with a decreased immune response from the stroma. The expression fold change of genes for secreted proteins in the stroma confirms this as significantly downregulated genes are almost entirely associated with inflammation (Supplemental Figure 7A). To determine if this reduction of inflammation-associated gene expression was the result of a change in the proportions of different stromal populations present in the tumor microenvironment, we looked at the expression of marker genes for endothelial cells, cancer associated fibroblasts, tumor associated macrophages, and neutrophils. For all cell types, few significant changes in marker gene expression were observed between SW480 Mock stroma and SW480 dnLEF1 stroma (Figure 4C, Supplemental Figure 7C–D), suggesting that the cellular composition of the overall tumor microenvironment is largely unchanged. We also used immunohistochemistry approaches to determine if patterns of localization and/or accumulation in around the tumor were different. F4/80 and Ly6g were used as markers of tumor associated macrophages and neutrophils, respectively, and CD31 was used

to mark endothelial cells (Figure 4D). Quantitation of positive staining cells from tissue sections showed that there was no significant change in the localization of tumor associated macrophages or neutrophils (Figure 4E–F). However, the localization of vessels revealed a significant shift from localization within the SW480 Mock tumor to the surrounding stroma in SW480 dnLEF1 tumors (Supplemental Figure 7E).

As changes in immune cell composition do not appear to account for the decrease in immune response in SW480 dnLEF1 tumors, we examined the expression of cytokines in the stroma and found that nearly all were significantly decreased in SW480 dnLEF1 stroma (Figure 4G, Supplemental Figure 7H). Cytokines were significantly increased in the SW620 dnLEF1 stroma (Supplemental Figure 8I). However, those increases derive from an extremely low baseline of expression in the SW620 Mock stroma, highlighting how even in the parental tumor these signatures of inflammation are low. Likewise, *NLRP3*, a key component of the innate immune response inflammasome is significantly downregulated in SW480 dnLEF1 stroma, consistent with a diminished immune response relative to the parental line (Figure 4H). Interestingly, multiple collagen genes in the stroma are less well expressed in SW480 dnLEF1 tumors compared to SW480 Mock tumors (Figure 4I–J, Supplemental Figure 7G), and they are differentially localized. Trichrome staining revealed a shift in collagen localization with strongly staining bundles of collagen deposition surrounding the tumor periphery of SW480 Mock tumors versus clear patterns of collagen integration into the SW480 dnLEF1 tumors (Supplemental Figure 7F). This finding is highly reminiscent of human CRC tumors with the low-Wnt, poor prognosis CMS4 tumor types having the highest levels of stromal infiltration (6). Similar stromal gene expression changes are observed in the SW620 dnLEF1 cells (Supplemental Figure 6I) and orthotopic tumors (Supplemental Figure 8A–J), though the stromal immune response is increased in the SW620 dnLEF1 orthotopic tumors. We hypothesize that this stromal change represents a different stage in tumor progression compared to the SW480 cell lines; as SW620 cells are inherently migratory, the diminished Wnt signal in this context pushes to advance metastasis rather than initiate it. These observations indicate that decreasing Wnt signaling in colon cancer cells leads to increased cell migration and invasion in a dosage-dependent manner relative to the magnitude of Wnt signal decrease, through both autocrine and paracrine signaling. In order to initiate the process of metastasis, the Wnt-decreased tumors orchestrate a weaker, diminished immune response while activating processes of tumor angiogenesis and matrix remodeling (Figure 5A).

Decreased Wnt signaling in colorectal cancer patients is correlated with poor prognosis

Recent attempts to categorize colorectal cancer patients by molecular biomarkers have consistently shown that patients with the highest levels of Wnt signaling have the best prognosis, and patients with the lowest levels have the poorest (6,9). To determine if our observations with decreased Wnt signaling in orthotopic tumors translated to the patient experience, we classified TCGA-COAD samples for CMS subtypes using the classifier described in Guinney et al. and performed GSEA to compare CMS2 (Wnt-high; best patient outcomes) to CMS4 (Wnt-low; poorest outcomes) samples. We found that the NLRP3 inflammasome is significantly enriched in CMS2 patients compared to CMS4, supporting our finding that Wnt-low tumors exhibit decreased expression of genes associated with an

immune response (Figure 5B). Additionally, we found the genes upregulated in SW480 dnLEF1 orthotopic tumors were enriched in CMS4 patients (Figure 5C). Lastly, we combined the significantly upregulated genes for secreted proteins expressed by both the tumor and stroma and found them to be collectively enriched in CMS4 patients (Figure 5D), suggesting that the signaling microenvironment that we modeled is most similar to the patients with the poorest outcomes.

These associations suggest that the signaling changes we observed in the tumor and tumor microenvironment could be used as predictors of patient outcomes. To test this, we identified the genes encoding secreted proteins that were significantly downregulated in SW480 dnLEF1 stroma and created interaction networks of known protein-protein interactors from STRING (30) that were expressed in the stroma. This process led to the identification of two stromal gene networks – one consisting of cytokines *CXCL1*, *CXCL2*, *CXCL3* and matrix metalloproteases *MMP9* and *MMP12*, and one consisting of inflammation activators *IL1A*, *IL1B*, *NLRP3*, and the innate immune response gene *LCN2*. We used publicly available datasets of colon cancer patients from GSE17538, GSE39582, GSE41258, and TCGA-COAD to identify patients with high or low expression of each gene network and found that high expression of the cytokine-metalloprotease network significantly predicted better patient outcomes, while the inflammation network did not have significant predictive power (Figure 5E).

We repeated the network analysis to identify signaling networks of genes for secreted proteins significantly upregulated in SW480 dnLEF1. From this process we identified four tumor gene networks: i) *AXL-GAS6*, a well-characterized ligand-tyrosine kinase receptor interaction that activates cell migration (42,43), ii) *CTHRC1*, a migration promoting gene previously linked to Wnt signaling activation (44,45) and two glycoproteins, *TPBG* and *GPC4*, iii) FN1 which has been implicated in promoting cell migration (46) with matrix remodeling glycoprotein *TNC*, and iv) a wound healing network consisting of plasminogen activator *PLAT*, coagulation factor *F10*, and EMT-promoting growth factor *MDK* (47). The *CTHRC1* and *FN1* networks did not significantly predict patient outcomes but high levels of expression of the *AXL-GAS6* and the wound healing network (*PLAT, F10, MDK*) were strong predictors of poor patient outcomes (Figure 5F). Thus, we conclude the cell signaling interactions found to be significantly changed in Wnt-decreased cell lines and tumors are predictive of poor patient outcomes for human CRC. These identified gene networks may point to therapeutic targets that may act synergistically with Wnt-targeting therapies which have had little success in colon cancer patients.

Discussion

Here we report that interfering with ß-catenin-dependent Wnt signaling in colon cancer cells increases their cell migration and invasion activities both *in vitro* and *in vivo*. We demonstrate this in multiple ways by interfering with Wnt signal transduction at steps that lie either upstream or downstream of ß-catenin. Wnt-signaling-inhibited cell lines show increased cell migration *in vitro*, a phenotype that correlates well with *in vivo* phenotypes of increased invasiveness, including the formation of extracolonic tumors. We predict that increased invasiveness would have been eventually manifest as metastases were we able to

carry out the experiments longer. However, the genetically manipulated cells are so invasive and aggressive at the primary site of injection in the caecum that the intestinal lumen was blocked and mice became moribund, therefore limiting the timeline of the study. We compared significantly upregulated genes in each of our lines to identify genes that are commonly upregulated when Wnt signaling is decreased, and discovered that a set of highly upregulated genes predicts poor outcomes in human CRC patients. We suggest that therapies targeting one or more of these genes may find clinical application in colon cancer patients presenting at the early stages of advanced disease.

Mutations that activate the Wnt signaling pathway have long been characterized as a hallmark of colon cancer, and multiple studies have pointed to the contribution of overactive Wnt signaling to metastatic disease. In patient samples, the leading edge of colon tumors stain strongly for nuclear ß-catenin, a marker of active Wnt signaling (48). Additionally, *SNAI1* and *TWIST1*, two genes that play key roles in EMT are direct Wnt target genes (49). Many previous studies have shown that decreasing Wnt signaling in colon cancer by targeting varying components of the pathway, can significantly reduce tumor burden in subcutaneous xenograft mouse models, the most common mouse model for pre-clinical testing of cancer therapeutics (34,50–53). Indeed, studies by our group using the dnLEF1 construct have shown the same result in subcutaneous xenografts (Fig. 1A–C), (16,54). Because of this, many efforts and deep resources have been brought to bear on the goal of bringing small molecule inhibitors of Wnt signaling into clinical practice. However, so far, none of these compounds have been able to show measurable benefit in colon cancer treatment, and the trials of Wnt inhibitors have shifted their focus to other cancer types (55). Recent evidence has shown that the genetic landscape of colon cancer is significantly more complex than previously appreciated; a meta-analysis of patient samples found that tumors with the lowest levels of Wnt signaling had the highest levels of stromal infiltration and the worst overall patient survival (6). By contrast, tumors with the highest levels of Wnt signaling had the best overall patient survival. The data that we present here supports this notion, and suggests that decreasing Wnt signaling directly favors an invasive phenotype in colon cancer.

One potential caveat is that both LEF1 and family member TCF1 (encoded by *TCF7*), can cooperate with ATF2 and ATF4 transcription factors to activate target genes in a beta-catenin-independent manner (56). We developed a lentiviral transduction system to produce moderate-to-low levels of dnLEF1 so as to avoid issues with overexpression (and only partially interfere with Wnt:beta-catenin), but we cannot formally rule out that some of the gene expression changes are due to a Wnt-independent activity of dnLEF1. To test whether this possibility was a dominant feature of our gene sets, we examined the expression of ATF2 target genes (57) and performed GSEA analysis on published ATF2 target genesets (58). We did not find any association between ATF2 and dnLEF1 regulation (Supplemental Figure 9A–B). We conclude that overall, dnLEF1 is primarily and directly enforcing changes on the Wnt target gene program.

Using gene ontology, we observe that Wnt interference in colon cancer cells by dnLEF1 expression is associated with enrichment for genes associated with epithelial to mesenchymal transition, loss of cell adhesion and invasion. We find that a high-level

of expression of these genes is significantly correlated with poorer patient outcomes in multiple patient data sets (Figure 5). The genes identified have been characterized to promote cell migration, either through changing gene expression or creating a more permissive extracellular matrix. Interestingly, RNAseq analysis of dnLEF1 expression in SW480 and SW620 cells cultured *in vitro* also showed changes in gene programs for cell adhesion, mobility, cell junction, and extracellular matrix (Supplemental Figure 8). However, the specific genes connected to these programs were different, showing that while the transcription programs and cell behaviors that link low Wnt signaling to invasive phenotypes is the same, the specific genes that change expression are different *in vitro* versus the orthotopic setting. Collectively, these programs highlight attempts by cancer cells to alter their microenvironment to promote invasion, as fibrotic, stiffened extracellular matrix has been shown to enhance EMT and invasion in many cancers (59).

Our findings suggest that high levels of Wnt signaling may indirectly repress invasive programs both in the tumors cells themselves and indirectly in the tumor microenvironment, fulfilling a specific role for strong Wnt signaling as an inhibitor of localized invasion. It is therefore possible that lower levels of Wnt signaling in APC-mutant colorectal cancer is linked to a colon cancer invasion-metastasis cascade and development of an invasion-promoting tumor microenvironment. Our results are concurrent with the CMS/CRIS colon cancer characterization studies and highlight how a decrease in Wnt signaling is an important contributing factor to advanced colon cancer and poor patient outcomes.

The ramifications of our findings are that while targeting Wnt signaling in colon cancer may reduce tumor burden, a potential, inadvertent side effect might be to induce surviving cancer cells to become invasive. Thus, as clinical trials continue to test the efficacy of newer, more specific Wnt inhibitors on Wnt-driven cancers, we suggest that treatment of patients with Wnt inhibitors should include concurrent treatment with drugs targeting one or more of the genes identified in this study, such as the *GAS6:AXL* pathway. In fact this pathway was recently reported to be increased in the invasive Stage IV of CRC (60). Autocrine Gas6:Axl signaling in the cancer cells can promote migration (60) and indeed there is three-fold more Axl expression in the invasive SW620 tumors compared to the SW480 tumors. Increased paracrine Gas6:Axl signaling is also likely to be highly significant, and for both SW480 and SW620 tumors, Gas6 is very highly expressed in the stroma. Several groups have shown the Gas6:Axl signal to be immune suppressive through a reduction in inflammation-promoting cytokines – which we also observe in our invasive tumors (61–63). Small molecule inhibitors have already been developed to target AXL and these have advanced to clinical trials. However, while AXL has been observed to be significantly overexpressed in malignant cells, none of the clinical trials currently testing AXL inhibitors are focused on colon cancer (42). We suggest that AXL inhibitors may be therapeutically useful in concert with other drug therapies, particularly Wnt or VEGF. Small molecule approaches targeting extracellular matrix proteins and related protein- and cell-ECM interactions have been found to have mixed clinical outcomes (59) – given our finding that such genes are upregulated in Wnt-low colon cancer, these small molecules may be prime candidates for combination with Wnt inhibitors.

Progression to metastatic disease remains the most challenging aspect of colon cancer treatment, and the one in which patient outcomes remain poor overall. The finding that these advanced tumors harbor relatively lower levels of Wnt signaling compared to other colon cancer subtypes, points to a previously uncharacterized role of Wnt signaling. Our study demonstrates that interference of Wnt/ß-catenin signaling activities induces a more invasive phenotype, and identifies a number of contributors to this invasive state. We suggest that future studies of Wnt inhibitors for clinical use consider concurrent treatment with inhibitors of these identified targets, to both reduce tumor burden and prevent cancer invasion.

Supplementary Material

Refer to Web version on PubMed Central for supplementary material.

Acknowledgments:

The authors would like to thank the members of the Waterman and Donovan labs for their scientific discussion and feedback, Melanie Oakes and Jenny Wu for bioinformatics assistance. We would also like to thank Emiliana Borrelli, Christopher Hughes, Arthur Lander, John Lowengrub, Harry Mangalam, Michael McClelland, Eric Pearlman, Eric Stanbridge, and Armando Villalta for providing advice and critiques.

Funding:

The work of G.T.C., Y.L., A.N.H., M.R.D., L.H., and M.L.W. was supported by NIH Grants CA096878, CA108697, a California CRCC award CRR-17-429379, R03CA223929, a U54CA217378 grant to the UCI Cancer Systems Biology Center (CaSB@UCI) and a P30CA062203 Cancer Center Support Grant to the Chao Family Comprehensive Cancer Center. G.T.C. was supported by NIH Grant CA200298. L.H. was supported by the NSF Graduate Research Fellowship Program under Grant DGE-1839285. The work of D.F.T. and R.A.E. were supported by P30CA062203, U54CA217378 and CRR-17-429379 to the Experimental Tissue Resource. This work was made possible in part, through access and support of the Genomics and High Throughput Facility and Flow Cytometry Core by the Cancer Center Support Grant (P30CA62203) and NIH shared instrumentation grants 1S10RR025496-01 and 1S10OD010794-01.

References:

1. Davis LE. The Evolution of Biomarkers to Guide the Treatment of Metastatic Colorectal Cancer. Am J Manag Care. 2018;24:107–17.
2. Voloshanenko O, Erdmann G, Dubash TD, Augustin I, Metzig M, Moffa G, et al. Wnt secretion is required to maintain high levels of Wnt activity in colon cancer cells. Nat Commun. Nature Publishing Group; 2013;4:2610. [PubMed: 24162018]
3. Seshagiri S, Stawiski EW, Durinck S, Modrusan Z, Storm EE, Conboy CB, et al. Recurrent R-spondin fusions in colon cancer. Nature. Nature Publishing Group; 2012;488:660–4. [PubMed: 22895193]
4. Aizawa T, Karasawa H, Funayama R, Shirota M, Suzuki T, Maeda S, et al. Cancer-associated fibroblasts secrete Wnt2 to promote cancer progression in colorectal cancer. Cancer Med. 2019;8:6370–82. [PubMed: 31468733]
5. Kramer N, Schmöllerl J, Unger C, Nivarthi H, Rudisch A, Unterleuthner D, et al. Autocrine WNT2 signaling in fibroblasts promotes colorectal cancer progression. Oncogene. 2017;36:5460–72. [PubMed: 28553956]
6. Guinney J, Dienstmann R, Wang X, de Reyniès A, Schlicker A, Soneson C, et al. The consensus molecular subtypes of colorectal cancer. Nat Med. 2015;21:1350–6. [PubMed: 26457759]
7. De Sousa E Melo F, Wang X, Jansen M, Fessler E, Trinh A, de Rooij LPMH, et al. Poor-prognosis colon cancer is defined by a molecularly distinct subtype and develops from serrated precursor lesions. Nat Med. Nature Publishing Group; 2013;19:614–8. [PubMed: 23584090]

8. de Sousa E Melo F, Colak S, Buikhuisen J, Koster J, Cameron K, de Jong JH, et al. Methylation of cancer-stem-cell-associated Wnt target genes predicts poor prognosis in colorectal cancer patients. Cell Stem Cell. Elsevier Inc.; 2011;9:476–85. [PubMed: 22056143]
9. Isella C, Brundu F, Bellomo SE, Galimi F, Zanella E, Porporato R, et al. Selective analysis of cancer-cell intrinsic transcriptional traits defines novel clinically relevant subtypes of colorectal cancer. Nat Commun. Nature Publishing Group; 2017;8:1–16. [PubMed: 28232747]
10. Arango D, Corner GA, Wadler S, Catalano PJ, Augenlicht LH. c-myc/p53 Interaction Determines Sensitivity of Human Colon Carcinoma Cells to 5-Fluorouracil in Vitro and in Vivo. Cancer Res. 2001;61:4910 LP–4915. [PubMed: 11406570]
11. Linnekamp JF, Van Hooff SR, Prasetyanti PR, Kandimalla R, Buikhuisen JY, Fessler E, et al. Consensus molecular subtypes of colorectal cancer are recapitulated in in vitro and in vivo models. Cell Death Differ. Springer US; 2018;25:616–33. [PubMed: 29305587]
12. Smedt L De, Palmans S, Govaere O, Boeckx B, Smeets D. Expression profiling of budding cells in colorectal cancer suggests an EMT-like phenotype and molecular subtype switching. Eur J Cancer. Nature Publishing Group; 2016;61:S88.
13. Seth C, Ruiz i Altaba A. Metastases and Colon Cancer Tumor Growth Display Divergent Responses to Modulation of Canonical WNT Signaling. PLoS One. 2016;11:e0150697. [PubMed: 26939070]
14. Varnat F, Siegl-Cachedenier I, Malerba M, Gervaz P, Ruiz i Altaba A. Loss of WNT-TCF addiction and enhancement of HH-GLI1 signalling define the metastatic transition of human colon carcinomas. EMBO Mol Med. 2010;2:440–57. [PubMed: 20941789]
15. Wenzel J, Rose K, Haghighi EB, Lamprecht C, Rauen G, Freihen V, et al. Loss of the nuclear Wnt pathway effector TCF7L2 promotes migration and invasion of human colorectal cancer cells. Oncogene. Springer US; 2020;
16. Pate KT, Stringari C, Sprowl-Tanio S, Wang K, TeSlaa T, Hoverter NP, et al. Wnt signaling directs a metabolic program of glycolysis and angiogenesis in colon cancer. EMBO J. 2014;33:1454–73. [PubMed: 24825347]
17. Najdi R, Proffitt K, Sprowl S, Kaur S, Yu J, Covey TM, et al. A uniform human Wnt expression library reveals a shared secretory pathway and unique signaling activities. Differentiation. Elsevier; 2012;84:203–13. [PubMed: 22784633]
18. Bankhead P, Loughrey MB, Fernández JA, Dombrowski Y, McArt DG, Dunne PD, et al. QuPath: Open source software for digital pathology image analysis. Sci Rep. 2017;7:16878. [PubMed: 29203879]
19. Picelli S, Faridani OR, Björklund ÅK, Winberg G, Sagasser S, Sandberg R. Full-length RNA-seq from single cells using Smart-seq2. Nat Protoc. 2014;9:171–81. [PubMed: 24385147]
20. Serra L, Chang D, Macchietto M, Williams K, Murad R, Lu D, et al. Adapting the Smart-seq2 Protocol for Robust Single Worm RNA-seq. BIO-PROTOCOL. 2018;
21. Bolger AM, Lohse M, Usadel B. Trimmomatic: a flexible trimmer for Illumina sequence data. Bioinformatics. 2014;30:2114–20. [PubMed: 24695404]
22. Conway T, Wazny J, Bromage A, Tymms M, Sooraj D, Williams ED, et al. Xenome-a tool for classifying reads from xenograft samples. Bioinformatics. 2012;28:i172–8. [PubMed: 22689758]
23. Frankish A, Diekhans M, Ferreira A-M, Johnson R, Jungreis I, Loveland J, et al. GENCODE reference annotation for the human and mouse genomes. Nucleic Acids Res. 2018;47:766–73.
24. Langmead B, Trapnell C, Pop M, Salzberg SL. Ultrafast and memory-efficient alignment of short DNA sequences to the human genome. Genome Biol. 2009;10.
25. Li B, Dewey CN. RSEM: Accurate transcript quantification from RNA-Seq data with or without a reference genome. BMC Bioinformatics. 2011;12.
26. Anders S, Huber W. Differential expression analysis for sequence count data. Genome Biol. 2010;11:R106. [PubMed: 20979621]
27. Ge SX, Jung D, Yao R. ShinyGO: a graphical gene-set enrichment tool for animals and plants. Bioinformatics. 2019;1–2.
28. Csardi G, Nepusz T. The igraph software package for complex network research. InterJournal, Complex Syst. 2006;1695:1–9.

29. Subramanian A, Tamayo P, Mootha VK, Mukherjee S, Ebert BL, Gillette MA, et al. Gene set enrichment analysis: A knowledge-based approach for interpreting genome-wide expression profiles. Proc Natl Acad Sci. 2005;102:15545 LP–15550. [PubMed: 16199517]
30. Szklarczyk D, Gable AL, Lyon D, Junge A, Wyder S, Huerta-Cepas J, et al. STRING v11: protein-protein association networks with increased coverage, supporting functional discovery in genome-wide experimental datasets. Nucleic Acids Res. 2019;47:D607–13. [PubMed: 30476243]
31. Smith JJ, Deane NG, Wu F, Merchant NB, Zhang B, Jiang A, et al. Experimentally derived metastasis gene expression profile predicts recurrence and death in patients with colon cancer. Gastroenterology. 2010;138:958–68. [PubMed: 19914252]
32. Marisa L, de Reyniès A, Duval A, Selves J, Gaub MP, Vescovo L, et al. Gene Expression Classification of Colon Cancer into Molecular Subtypes: Characterization, Validation, and Prognostic Value. Kemp C, editor. PLoS Med. 2013;10:e1001453. [PubMed: 23700391]
33. Sheffer M, Bacolod MD, Zuk O, Giardina SF, Pincas H, Barany F, et al. Association of survival and disease progression with chromosomal instability: a genomic exploration of colorectal cancer. Proc Natl Acad Sci U S A. 2009;106:7131–6. [PubMed: 19359472]
34. Van de Wetering M, Sancho E, Verweij C, De Lau W, Oving I, Hurlstone A, et al. The β-catenin/TCF-4 complex imposes a crypt progenitor phenotype on colorectal cancer cells. Cell. 2002;111:241–50. [PubMed: 12408868]
35. Lawson DA, Bhakta NR, Kessenbrock K, Prummel KD, Yu Y, Takai K, et al. Single-cell analysis reveals a stem-cell program in human metastatic breast cancer cells. Nature. 2015;526:131–5. [PubMed: 26416748]
36. Giannakis M, Hodis E, Jasmine Mu X, Yamauchi M, Rosenbluh J, Cibulskis K, et al. RNF43 is frequently mutated in colorectal and endometrial cancers. Nat Genet. 2014;3–5. [PubMed: 24370740]
37. Jung Y, Jun S, Lee SH, Sharma A, Park J. Wnt2 complements Wnt/β-catenin signaling in colorectal cancer. Oncotarget. 2015;6:37257–68. [PubMed: 26484565]
38. Nishioka M, Ueno K, Hazama S, Okada T, Sakai K, Suehiro Y, et al. Possible involvement of Wnt11 in colorectal cancer progression. Mol Carcinog. 2011;52:1–11. [PubMed: 22025467]
39. Goel S, Chin EN, Fakhraldeen S a, Berry SM, Beebe DJ, Alexander CM. Both LRP5 and LRP6 receptors are required to respond to physiological Wnt ligands in mammary epithelial cells and fibroblasts. J Biol Chem. 2012;287:16454–66. [PubMed: 22433869]
40. Saito-diaz K, Benchabane H, Tiwari A, Tian A, Li B, Joshua J, et al. APC Inhibits Ligand-Independent Wnt Signaling by the Clathrin Endocytic Pathway. Dev Cell. Elsevier Inc.; 2018;44:566–581.e8. [PubMed: 29533772]
41. Subramanian A, Tamayo P, Mootha V. GSEA: Gene set enrichment analysis Gene set enrichment analysis: A knowledge-based approach for interpreting genome-wide expression profiles. Pnsa. 2014;
42. Axelrod H, Pienta KJ. Axl as a mediator of cellular growth and survival. Oncotarget. 2014;5:8818–52. [PubMed: 25344858]
43. Goyette MA, Duhamel S, Aubert L, Pelletier A, Savage P, Thibault MP, et al. The Receptor Tyrosine Kinase AXL Is Required at Multiple Steps of the Metastatic Cascade during HER2-Positive Breast Cancer Progression. Cell Rep. 2018;23:1476–90. [PubMed: 29719259]
44. Yang XM, You HY, Li Q, Ma H, Wang YH, Zhang YL, et al. CTHRC1 promotes human colorectal cancer cell proliferation and invasiveness by activating Wnt/PCP signaling. Int J Clin Exp Pathol. 2015;8:12793–801. [PubMed: 26722469]
45. Kim HC heo., Kim YS un., Oh HW, Kim K, Oh SS, Kim JT, et al. Collagen triple helix repeat containing 1 (CTHRC1) acts via ERK-dependent induction of MMP9 to promote invasion of colorectal cancer cells. Oncotarget. 2014;5:519–29. [PubMed: 24504172]
46. Pupa SM, Ménard S, Forti S, Tagliabue E. New insights into the role of extracellular matrix during tumor onset and progression. J Cell Physiol. 2002;192:259–67. [PubMed: 12124771]
47. Filippou PS, Karagiannis GS, Constantinidou A. Midkine (MDK) growth factor: a key player in cancer progression and a promising therapeutic target. Oncogene. Springer US; 2020;39:2040–54. [PubMed: 31801970]

48. Jung A, Schrauder M, Oswald U, Knoll C, Sellberg P, Palmqvist R, et al. The Invasion Front of Human Colorectal Adenocarcinomas Shows Co-Localization of Nuclear β-Catenin, Cyclin D1, and p16INK4A and Is a Region of Low Proliferation. Am J Pathol. 2001;159:1613–7. [PubMed: 11696421]
49. ten Berge D, Koole W, Fuerer C, Fish M, Eroglu E, Nusse R. Wnt Signaling Mediates Self-Organization and Axis Formation in Embryoid Bodies. Cell Stem Cell. Elsevier Inc.; 2008;3:508–18. [PubMed: 18983966]
50. Morin PJ, Vogelstein B, Kinzlertt KW. Apoptosis and APC in colorectal tumorigenesis. Med Sci. 1996;93:7950–4.
51. Satoh S, Daigo Y, Furukawa Y, Kato T, Miwa N, Nishiwaki T, et al. AXIN1 mutations in hepatocellular carcinomas, and growth suppression. Nat Genet. 2000;24:245–50. [PubMed: 10700176]
52. Tetsu O, McCormick F. Beta-catenin regulates expression of cyclin D1 in colon carcinoma cells. Nature. 1999;398:422–6. [PubMed: 10201372]
53. Polakis P Drugging Wnt signalling in cancer. EMBO J. Nature Publishing Group; 2012;31:2737–46. [PubMed: 22617421]
54. Lee M, Chen GT, Puttock E, Wang K, Edwards RA, Waterman ML, et al. Mathematical modeling links Wnt signaling to emergent patterns of metabolism in colon cancer. Mol Syst Biol. 2017;13:912. [PubMed: 28183841]
55. Kahn M Can we safely target the WNT pathway? Nat Rev Drug Discov. Nature Publishing Group; 2014;13:513–32. [PubMed: 24981364]
56. Grumolato L, Liu G, Haremaki T, Mungamuri SK, Mong P, Akiri G, et al. β-Catenin-Independent Activation of TCF1/LEF1 in Human Hematopoietic Tumor Cells through Interaction with ATF2 Transcription Factors. PLOS Genet. Public Library of Science; 2013;9:e1003603. [PubMed: 23966864]
57. Watson G, Ronai ZA, Lau E. ATF2, a paradigm of the multifaceted regulation of transcription factors in biology and disease. Pharmacol Res. 2017/02/15. 2017;119:347–57. [PubMed: 28212892]
58. Bailey J, Tyson-Capper AJ, Gilmore K, Robson SC, Europe-Finner GN. Identification of human myometrial target genes of the cAMP pathway: the role of cAMP-response element binding (CREB) and modulator (CREMalpha and CREMtau2alpha) proteins. J Mol Endocrinol. England; 2005;34:1–17. [PubMed: 15691874]
59. Kai FB, Drain AP, Weaver VM. The Extracellular Matrix Modulates the Metastatic Journey. Dev Cell. Elsevier Inc.; 2019;49:332–46. [PubMed: 31063753]
60. Uribe DJ, Mandell EK, Watson A, Martinez JD, Leighton JA, Ghosh S, et al. The receptor tyrosine kinase AXL promotes migration and invasion in colorectal cancer. PLoS One. 2017;12:1–16.
61. Dunne PD, McArt DG, Blayney JK, Kalimutho M, Greer S, Wang T, et al. AXL Is a Key Regulator of Inherent and Chemotherapy-Induced Invasion and Predicts a Poor Clinical Outcome in Early-Stage Colon Cancer. Clin Cancer Res. 2014;20:164 LP–175. [PubMed: 24170546]
62. Rothlin C V, Ghosh S, Zuniga EI, Oldstone MBA, Lemke G. TAM Receptors Are Pleiotropic Inhibitors of the Innate Immune Response. Cell. 2007;131:1124–36. [PubMed: 18083102]
63. Tanaka M, Siemann DW. Gas6/Axl Signaling Pathway in the Tumor Immune Microenvironment. Cancers . 2020.
64. Edgar R, Domrachev M, Lash AE. Gene Expression Omnibus: NCBI gene expression and hybridization array data repository Nucleic Acids Res. 2002 Jan 1;30(1):207–10 [PubMed: 11752295]

Implications:

Decreased Wnt signaling in colon tumors leads to a more aggressive disease phenotype due to an upregulation of gene programs favoring cell migration in the tumor and downregulation of inflammation programs in the tumor microenvironment; these impacts must be carefully considered in developing Wnt-targeting therapies.

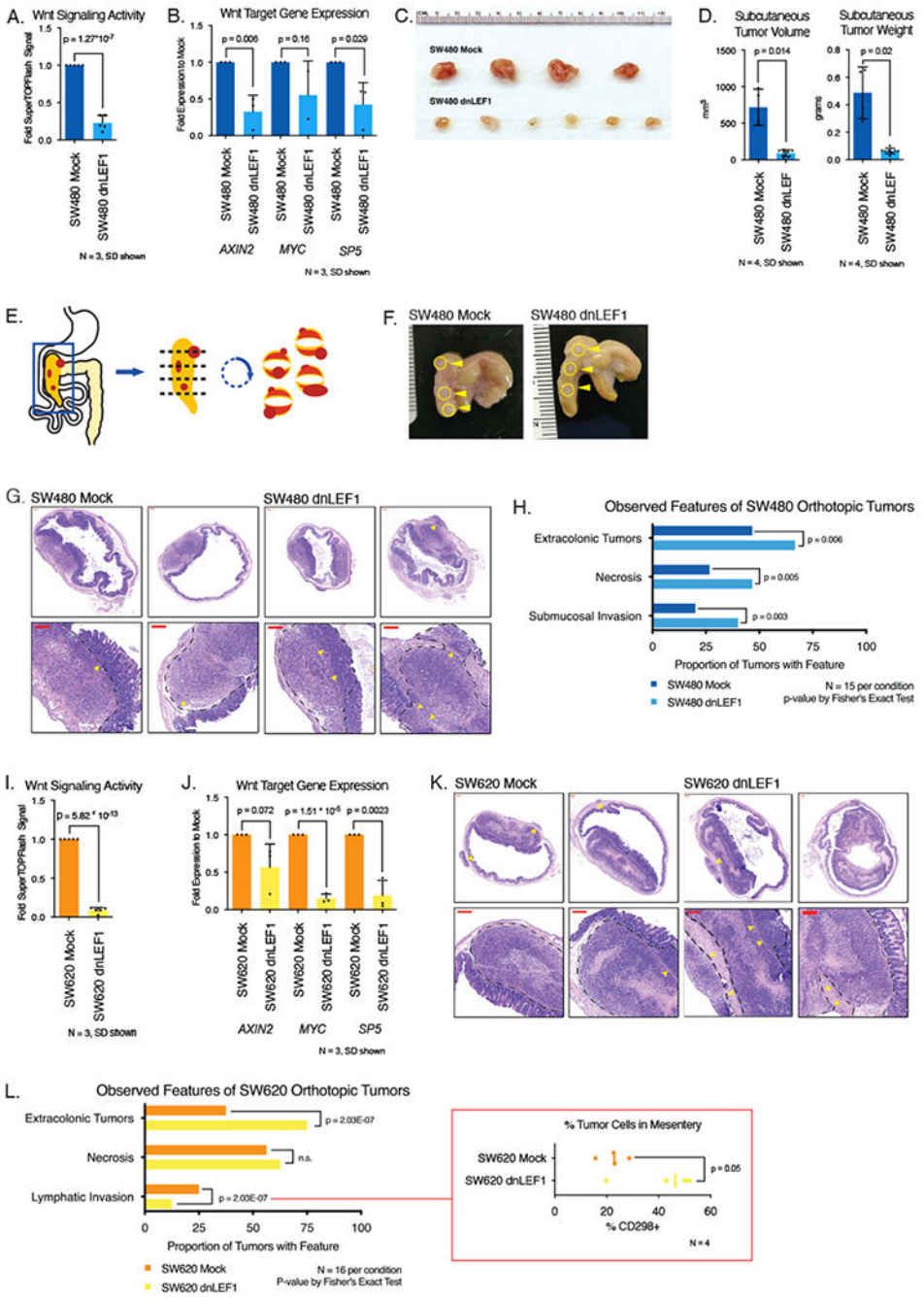

Figure 1. Decreasing Wnt in SW480 and SW620 colon cancer xenografts increases cell migration and invasion.

A. dnLEF1-transduced SW480 cells show a significant decrease in Wnt signaling activity as measured by SuperTOPFlash luciferase reporter activity.

B. Expression of Wnt target genes *AXIN2*, *MYC*, and *SP5* are decreased by dnLEF1 expression in SW480 cells as measured by quantitative PCR.

C. SW480 dnLEF1 cells show a significant decrease in tumor burden compared to SW480 Mock cells in subcutaneous tumors in immunocompromised mice. Representative images of subcutaneous tumors at harvest.

D. Quantitation of both tumor volume and weight show statistically significant differences between SW480 Mock and SW480 dnLEF1.

E. Schematic of orthotopic injection and harvest. Tumors are injected into the caecum wall and allowed to grow for 3-5 weeks. At harvest, the caecum is cut on the latitude and mounted on edge.

F. SW480 Mock and SW480 dnLEF1 cells show no significant difference in orthotopic tumor size. Representative images of caecums at harvest. Scale bar is in millimeters.

G. Formalin fixed, paraffin embedded (FFPE) sections of SW480 Mock and SW480 dnLEF1 orthotopic tumors stained with hematoxylin and eosin. Top row: full caecum section, bottom row: magnified inset. All scale bars 200um. Dotted lines outline the tumor border, arrowheads mark the invasive edge.

H. Blinded scoring of orthotopic tumor sections shows a significant increase in extracolonic tumors, necrotic area, and submucosal invasion in caecums injected SW480 dnLEF1 cells compared to SW480 Mock.

I. dnLEF1-transduced SW620 cells show a significant decrease in Wnt signaling activity as measured by SuperTOPFlash luciferase reporter activity.

J. Expression of Wnt target genes *AXIN2*, *MYC*, and *SP5* are decreased by dnLEF1 expression in SW620 cells as measured by quantitative PCR.

K. FFPE sections of SW620 Mock and SW620 dnLEF1 orthotopic tumors stained with hematoxylin and eosin. Dotted lines outline the tumor border, arrowheads mark the invasive edge. Top row: full caecum section, bottom row: magnified inset. All scale bars 200um.

L. Blinded scoring of orthotopic tumor sections shows a significant increase in extracolonic tumors in SW620 dnLEF1 tumors compared to SW480 Mock, but no significant increase in necrosis, and a decrease in lymphatic invasion. (Inset) Flow cytometry analysis of CD298+ cells in the mouse mesentery shows a significant increase in circulating tumor cells in SW620 dnLEF1-injected mice compared to SW620 Mock-injected mice.

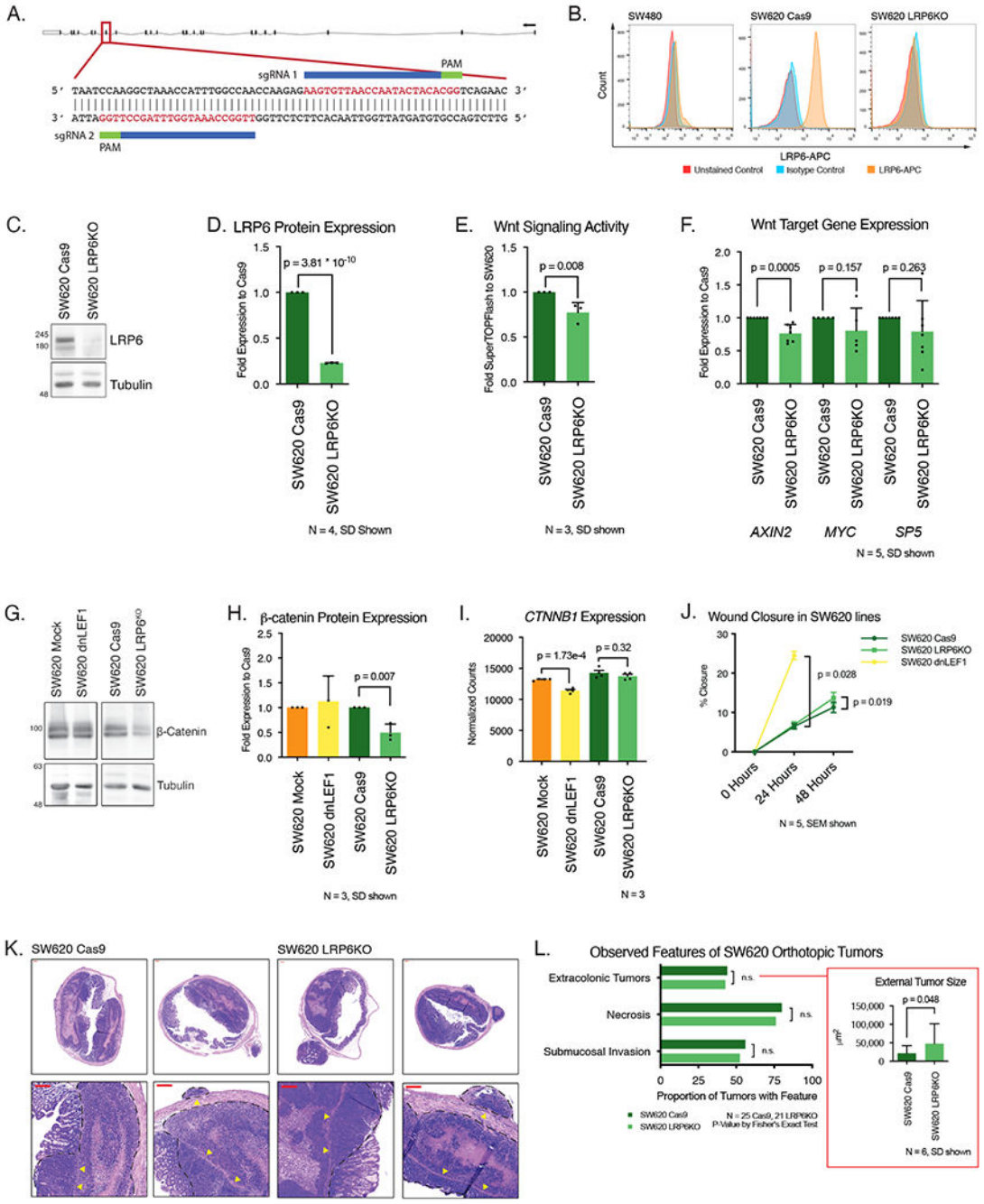

Figure 2. Modulating Wnt signaling upstream or downstream of b-catenin in SW620 cells increases invasion in orthotopic tumors.

A. Schematic for LRP6 CRISPR guide RNA design. Two CRISPR guide RNAs were developed to target LRP6, their alignments to the nucleotide sequence along with the PAM sites are highlighted in the blue bar. Both guide RNAs were used with a Cas9 nickase for specific targeting of LRP6.

B. Live cell flow cytometry reveals minimal expression of LRP6 in SW480 cells at the cell membrane, but is visible when cells are fixed (Supplemental Figure 3). In contrast, SW620

cells robustly express LRP6, and LRP6 CRISPR expression, coupled with FACS sorting and clonal expansion, successfully eliminated LRP6 protein from the cell membrane.

C-D. Validation of LRP6 knockout in SW620 by Western blotting shows a significant decrease in total protein level.

E. LRP6 knockout in SW620 cells induced a modest, but statistically significant decrease in Wnt signaling activity as measured by SuperTOPFlash luciferase activity.

F. Expression of Wnt target genes *AXIN2*, *MYC*, and *SP5* in SW620 LRP6KO normalized to parental control. *AXIN2* is significantly decreased; *MYC* and *SP5* trend downwards but not to significance.

G-I. Total ß-catenin protein level is significantly decreased in SW620 LRP6KO, but not SW620 dnLEF1. The loss of LRP6 affects the stability of ß-catenin due to the release of the destruction complex from the plasma membrane (40). *CTNNB1* mRNA is not significantly decreased in SW620 LRP6KO compared to SW620 Cas9.

J. Scratch assay of SW620 Cas9, SW620 LRP6KO, and SW620 dnLEF1 cells shows a significant difference in cell motility after 24 hours for SW620 dnLEF1, after 48 hours for SW620 LRP6KO, suggesting with a more dramatic Wnt inhibition, there is an increase in cell motility.

K. Representative hematoxylin & eosin stained sections of SW620 Cas9 and SW620 LRP6KO orthotopic tumors. Top row: full caecum section, bottom row: magnified inset. Scalebars are 200um. Dotted lines outline tumor, arrowheads mark invasive edge.

L. Blinded scoring of SW620 Cas9 and SW620 LRP6KO orthotopic tumor sections. Quantification of extracolonic tumors per section shows no difference in number of extracolonic tumors between SW620 Cas9 and SW620 LRP6KO. Area measurements of extracolonic tumors show a significantly higher average extracolonic tumor size in SW620 LRP6KO sections.

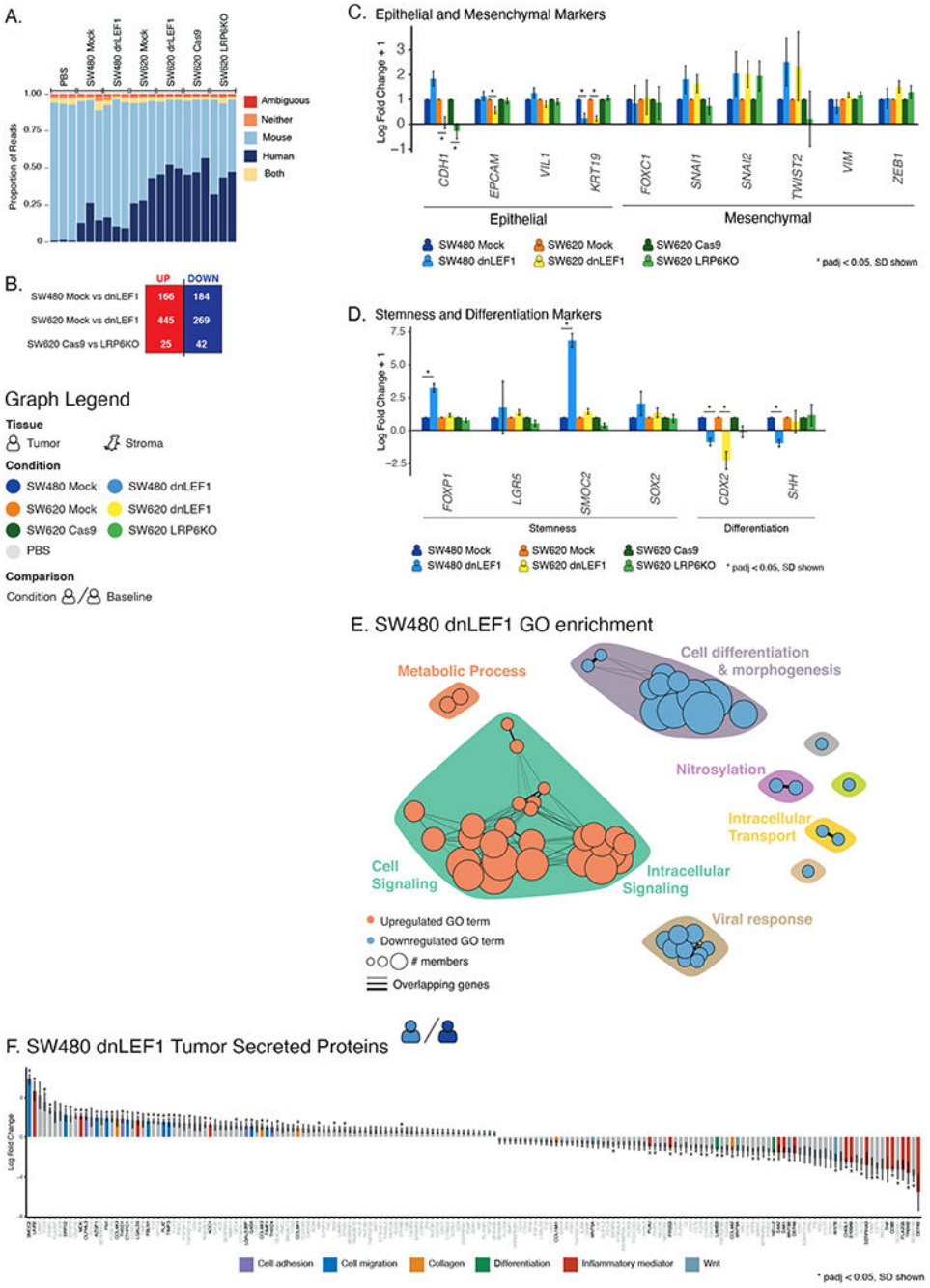

Figure 3. RNA sequencing of orthotopic tumors reveals an increase in stemness gene expression and increase expression of migration-promoting signaling genes with decreasing Wnt signaling levels.

A. Proportion of reads from orthotopic tumor samples mapped to mouse or human genomes. Proportion of human to mouse reads can be considered as proxy for proportion of tissue from each species in each sample.

B. Differentially expressed genes reaching significance of $p > 0.05$ in comparing parental tumors to Wnt-reduced tumors in human genome.

C. Expression of marker genes for epithelial and mesenchymal cells shows a trend towards decreased expression of epithelial markers and increased expression of mesenchymal markers with decreasing Wnt activity.

D. Expression of marker genes for stemness and differentiation shows a significant increase in stemness genes and decrease in differentiation genes with decreasing Wnt activity in SW480 tumors but not SW620 tumors.

E. Network graph of significantly upregulated and downregulated gene ontology (GO) terms in SW480 dnLEF1 tumors compared to SW480 Mock tumors. Each GO term is scaled by number of genes represented in list. Line density indicates number of overlapping genes between GO terms. Terms are clustered in terms of similarity to identify a meta GO term. SW480 dnLEF1 tumors show an upregulation of processes associated with cell signaling and a downregulation of programs associated with differentiation.

F. Differential expression of genes encoding secreted proteins between SW480 dnLEF1 and SW480 Mock tumors show an upregulation of cell migration-promoting genes and a downregulation of inflammatory response genes.

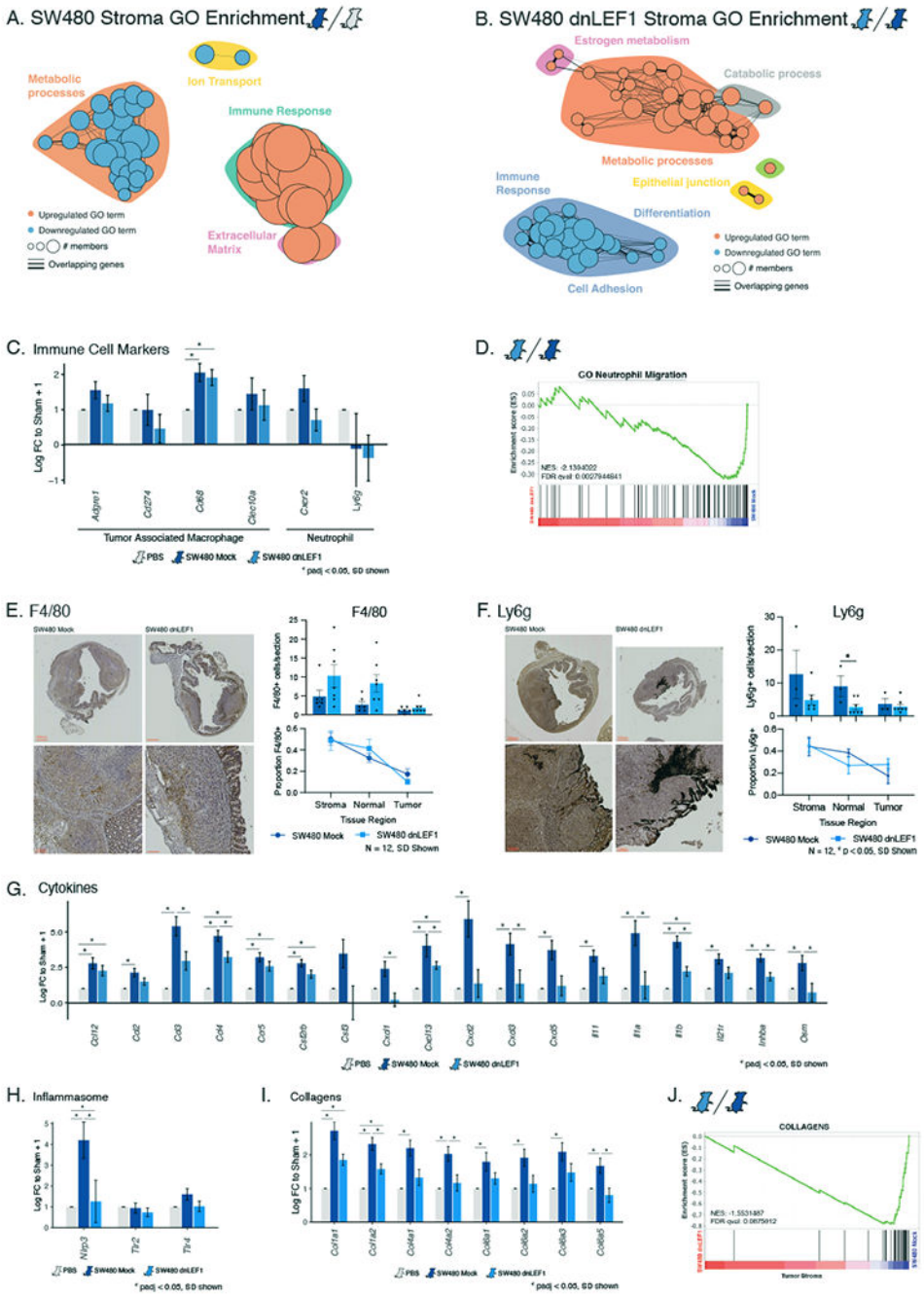

Figure 4. RNA sequencing of orthotopic tumor stroma cells reveals a decreased immune response and altered extracellular matrix in response to orthotopic injection of SW480 dnLEF1 cells.

A. Gene Ontology network of significantly upregulated and downregulated genes between SW480 Mock stroma and sham-injected stroma reveals an enrichment of Immune Response related GO terms.

B. Gene Ontology of significantly upregulated and downregulated genes between SW480 dnLEF1 stroma and SW480 Mock stroma shows a downregulation of terms associated with immune response, cell adhesion, and differentiation.

C. Expression of immune cell markers in mouse stroma suggest no significant changes in proportions of Tumor Associated Macrophages or Neutrophils between sham injected, SW480 Mock-injected, or SW480 dnLEF1-injected stroma.

D. Gene set enrichment analysis (GSEA) identifies a significant downregulation of Neutrophil Migration genes in SW480 dnLEF1 stroma compared to SW480 Mock.

E. Representative IHC and quantitation of TAM marker F4/80 (Adgre1) expression in orthotopic tumor sections. Scalebars are 200um. Equally sized sections of tumor, stroma, and normal epithelia were counted by blinded observers. No significant difference in TAM cell number and localization is seen between SW480 Mock and SW480 dnLEF1 orthotopic tumors.

F. Representative IHC and quantitation of neutrophil marker Ly6g in SW480 Mock or SW480 dnLEF1 orthotopic tumor sections. Scalebars are 200um. Equally sized sections of tumor, stroma, and normal epithelia were counted by blinded observers. No significant difference in neutrophil localization is seen between SW480 Mock and SW480 dnLEF1 orthotopic tumors. A significant decrease in cell number is only observed in the normal epithelial of SW480 dnLEF1 orthotopic tumors.

G. Cytokine expression is significantly upregulated with SW480 Mock injection, but not SW480 dnLEF1 expression compared to sham.

H. *NLRP3* is significantly upregulated in SW480 Mock stroma but is not changed in SW480 dnLEF1 stroma.

I. Collagens are significantly upregulated in SW480 Mock stroma relative to sham but downregulated in SW480 dnLEF1 stroma.

J. GSEA of collagen genes shows a significant collective downregulation of collagens in SW480 dnLEF1 stroma compared to SW480 Mock.

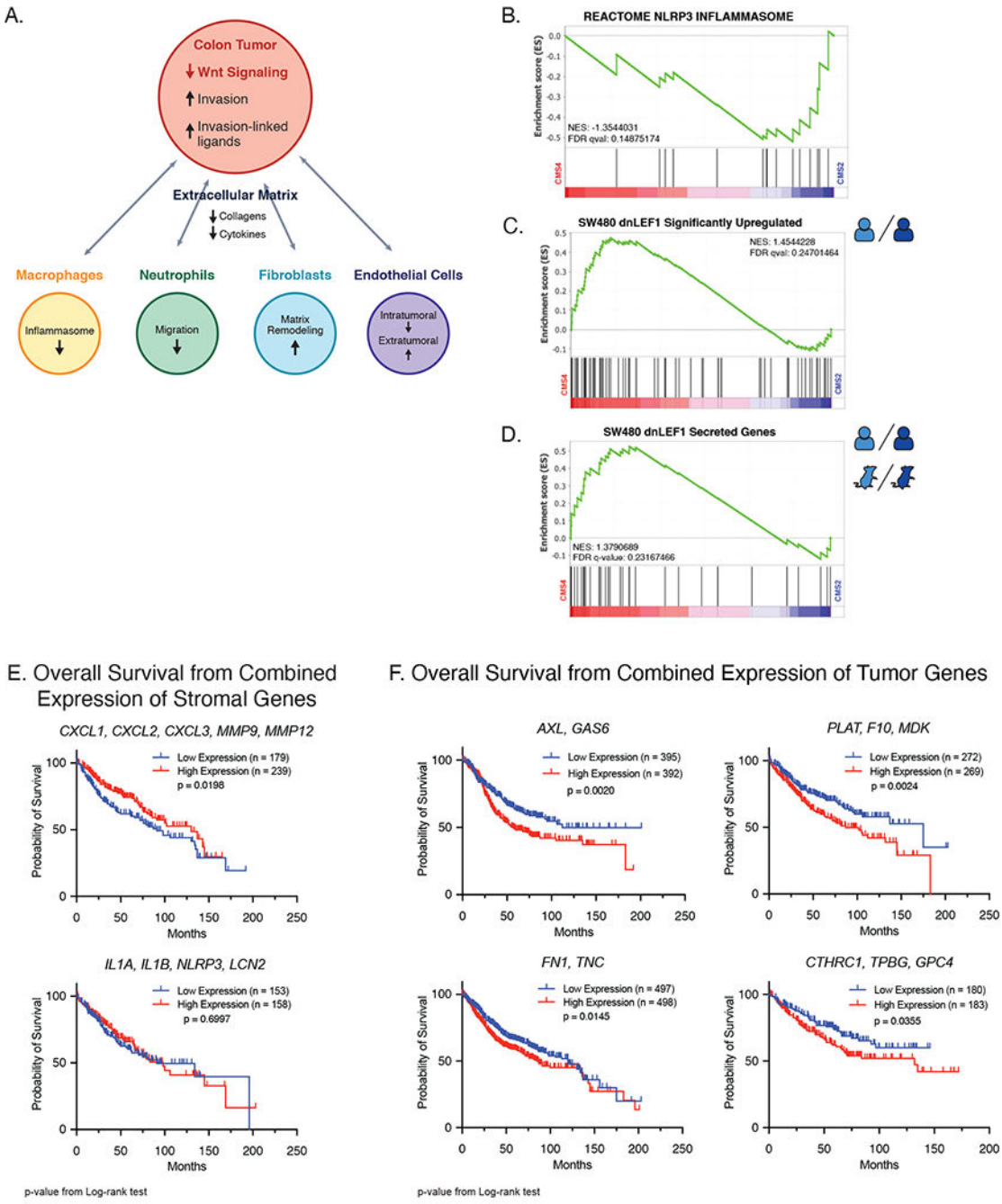

Figure 5. Decreased Wnt signaling in colon cancer cells is correlated with a decreased immune response and increased matrix remodeling and reflects poor patient survival.

A. Our working model describes how decreasing Wnt signaling in colon cancer cells elicits a change in response from the surrounding extracellular matrix that facilitates tumor invasion.

B. GSEA of NLRP3 inflammasome genes shows an enrichment in TCGA-COAD patients identified to the Wnt-high CMS2 molecular subtype compared to Wnt-low CMS4 patients.

C. GSEA of significantly upregulated genes in SW480 dnLEF1 tumor cells show an enrichment in CMS4 patients compared to CMS2.

D. GSEA of secreted genes from both SW480 dnLEF1 stroma and tumor are enriched in CMS4 patients compared to CMS2.

E. Kaplan-Meier analysis of overall survival in colon cancer patients from GSE17538, GSE39582, GSE41258, and TCGA-COAD for gene sets found to be downregulated in SW480 dnLEF1 stroma compared to SW480 Mock. Gene sets were determined by significant differential expression of secreted genes and expressed genes of known interactors. High expression of identified gene sets is predictive of better patient survival. After Bonferroni correction, the *CXCL* & *MMP*-linked sets remains significant at a p value < 0.025.

F. Kaplan-Meier analysis of overall survival in colon cancer patients from GSE17538, GSE39582, GSE41258, and TCGA-COAD for gene sets found to be upregulated in SW480 dnLEF1 orthotopic tumors compared to SW480 Mock. High expression of identified gene sets is predicted of poor patient survival. After Bonferroni correction, the *AXL* and *PLAT*-linked sets remain significant at a p-value < 0.0125.